Methylation of Ir(III)-tetrazolato complexes: an effective route to modulate the emission outputs and to switch to antimicrobial properties.

Valentina Fiorini,[a] Ilaria Zanoni,[a,b] Stefano Zacchini,[a] Anna Luisa Costa,[b] Alejandro Hochkoeppler,[c,e] Valerio Zanotti,[a] Anna Maria Ranieri,[d] Massimiliano Massi,[d]* Alessandra Stefan[c,e]* and Stefano Stagni[a]*

a: Department of Industrial Chemistry "Toso Montanari", University of Bologna, Viale Risorgimento 4, I-40136 Bologna, Italy.

b: CNR-ISTEC- National Research Council of Italy, Institute of Science and Technology for Ceramics, Via Granarolo 64 I-48018, Faenza (RA), Italy.

c: Department of Pharmacy and Biotechnology, University of Bologna, Viale Risorgimento 4, I-40136 Bologna, Italy.

d: Nanochemistry Research Institute, Department of Chemistry, Curtin University, GPO Box U 1987, Perth, Australia 6845.

e: CSGI, University of Florence, Via della Lastruccia 3, 50019 Sesto Fiorentino (FI), Italy.

Email: stefano.stagni@unibo.it (Stefano Stagni); alessandra.stefan@unibo.it (Alessandra Stefan); M.Massi@curtin.edu.au (Massimiliano Massi)

Abstract

Two neutral cyclometalated Ir(III)-tetrazolato complexes that differ by variations of the substituents on either the phenylpyridine or tetrazolate ligand, have been converted into the corresponding methylated and cationic analogues. The NMR (^{1}H, ^{13}C) characterization of the Ir(III) complexes provided results in agreement with the chemo- and regioselective character of the methylation at the N-3 position of the Ir(III)-coordinated tetrazolato ring. This evidence was further corroborated by the analysis of the molecular structures of the cationic complexes obtained by X-ray diffraction. From the stand point of the photophysical properties, the addition of a methyl moiety to neutral Ir(III) tetrazolates, which behave as sky-blue or orange phosphors, caused the systematic red shift of their phosphorescence output. The transformation of neutral Ir(III) tetrazolates into cationic Ir(III)-tetrazole complexes was screened for any eventual antimicrobial activity *in vitro* against Gram negative (*E. coli*) and Gram positive (*D. radiodurans*) microorganisms. Whereas both kind of complexes were not active against *E. Coli*, the conversion of the neutral Ir(III) tetrazolates into the corresponding methylated and cationic Ir(III)tetrazole derivatives, determined the turn-on of a good to excellent antimicrobial activity toward Gram positive *Deinococcus radiodurans*, a not pathogenic bacterium that is listed as one of the toughest microorganisms in light of its outstanding resistance to radiation and oxidative stress.

Introduction

Since the past two decades, Ir(III) cyclometalated complexes have been in the spotlight of the research programs of many groups worldwide.[1] Such a pronounced and still active scientific interest reflects the multiple applications of this class of compounds in research themes that have in common the study of the interaction of matter with light. Following the fundamental studies centred on the photophysics of Ir(III) cyclometalates, these molecules have emerged as the paradigm of the metal-based phosphors for lighting devices, foldable displays and, in general, for all the applications in which bright and colour tuneable emissions are required.[2] Also, the characteristic photoluminescent output displayed by these molecules has allowed their use as responsive chemosensors,[3] promising photocatalysts[4] and luminescent markers for live cell imaging.[5]

On the other hand, in comparison to isoelectronic Ru(II)-polypyridyls[6] and many other classes of metal-based derivatives,[7] including organometallic and "classical" Ag(I)-based coordination compounds,[8] the antimicrobial properties of Ir(III) complexes have been explored to a lesser extent.[9] In this regard, in a very recent report Chao and coworkers have for the first time demonstrated the promising anti microbial potential of a set of kinetically stable and substitution inert cationic Ir(III) cyclometalated complexes towards Gram (+) bacteria (*e.g Staphylococcus aureus*),[10] adding therefore further possibilities for the application of this class of luminescent compounds.

Within the framework of our studies dealing with luminescent metal complexes containing 5 aryl tetrazolate ligands,[11] we have dedicated much attention to the corresponding heteroleptic Ir(III) cyclometalates with the general formula $Ir(C^N)_2(N^N)]$,[12] where C^N is represented by the cyclometalating 2-phenylpyridine (ppy) or 2-(2,4-difluorophenyl)pyridine (F_2ppy) and N^N denotes tetrazolate ligands. The inclusion of these anionic and nitrogen rich ligands in the structure of such Ir(III) chelates led to a family of neutrally charged complexes in which a significant tuning of the luminescence maxima could be accomplished upon simple chemical modulation of the tetrazolato ancillary ligand. In the biological context, we have recently investigated the use of these neutral Ir(III) tetrazolate complexes as luminescent markers for live cells imaging. As a direct comparison, we have also explored the corresponding cationic complexes that were obtained by irreversible methylation of the neutral iridium species, according to the peculiar reactivity of the coordinated tetrazolate ring toward electrophiles. [12, 13, 14, 15] From this study, an interesting trend has emerged, illustrating how while the neutral iridium complexes display low levels of adverse effects,

methylation causes systematic enhancement of cytotoxicity.[16] This behaviour seems to mostly originate from the specific localisation of the iridium complexes within the cells, with the cationic complexes predominantly targeting the mitochondria. Furthering these studies, we have now selected two Ir(III)-tetrazolates (Scheme 1) that display different luminescent outputs and focused our attention to the antibacterial properties of these iridium complexes and in particular, to the potential differences between the neutral and charged species. The results reported herein highlight an analogous behaviour, with a "switch on" of their antimicrobial activity toward Gram (+) *Deinococcus radiodurans*, which is one of the most resistant bacteria featuring appropriate defence systems against oxidative damage,[17] upon methylation of the parent neutral Ir(III)complexes.

Results and discussion

The synthetic procedure for the preparation of the target complexes is illustrated in Scheme 1.

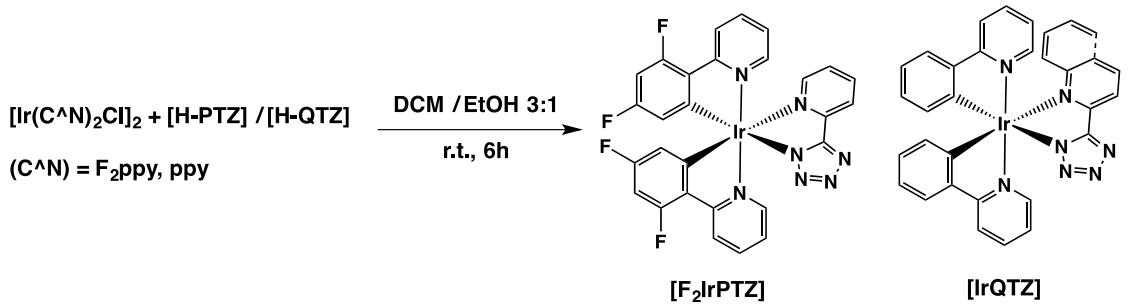

Scheme 1: Synthetic procedure used for the preparation of neutral Ir(III) complexes discussed in this work.

The neutral Ir-cyclometalates **[F_2IrPTZ]** and **[IrQTZ]**[16] were obtained by the standard method involving the reaction of the appropriate tetrazole, namely H-PTZ and H-QTZ, with the Ir(III) chloride bridged dimers.[12a, 15] In a successive stage, the neutral Ir(III) tetrazolates **[F_2IrPTZ]** and **[IrQTZ]** were treated with methyl triflate (Scheme 2) to afford the corresponding Ir(III)-tetrazole cationic complexes **[F_2IrPTZ-Me]$^+$** and **[IrQTZ-Me]$^+$**, which were recovered as the hexafluorophosphate salts following a metathesis procedure. [12a, 15]

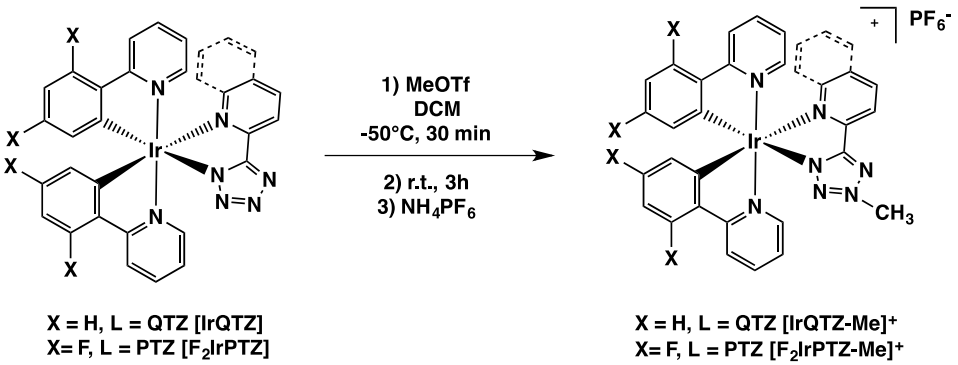

Scheme 2: Synthetic procedure used for the preparation of cationic Ir(III) complexes discussed in this work.

The formation of the target complexes was at first verified by Electro Spray Ionization Mass Spectrometry (ESI-MS, see ESI Fig. S1-4) and the subsequent NMR (^{1}H, ^{13}C) characterization suggested the occurrence of the expected Ir(III) chelate complexes with C_s symmetry (See ESI Fig S5-11). In perfect agreement with our past works dealing with structurally similar Ru(II) and Ir(III)tetrazolate complexes,[11, 12, 15] the deeper analysis of the ^{1}H and, in particular, of the ^{13}C NMR spectra of neutral and cationic Ir(III) complexes described herein suggest the coordination of the tetrazolate (complexes **[F_2IrPTZ]** and **[IrQTZ]**) or tetrazole ring (complexes **[F_2IrPTZ-Me]$^+$** and **[IrQTZ-Me]$^+$**) through the N-1 position. Also, the subtle but clearly distinguishable downfield

shifting of the tetrazolic carbon that is observed upon the conversion of the neutral complexes into their corresponding methylated and positively charged analogues **[F$_2$IrPTZ-Me]$^+$** and **[IrQTZ-Me]$^+$**suggests the regioselective addition of the methyl group to the less sterically demanding N-3 position of the Ir(III)-coordinated tetrazolate ring.[12, 15]

All these evidences were further corroborated by the analysis of the unprecedented molecular structures obtained by X-ray diffraction of **[IrQTZ]**, **[IrQTZ-Me]$^+$** and **[F$_2$IrPTZ-Me]$^+$** (Figures 1-3). In all the complexes the tetrazole ring is coordinated through the N-1 position and methylation of **[IrQTZ-Me]$^+$** and **[F$_2$IrPTZ-Me]$^+$** occurs at N-3. The N atoms of the cyclometalated ligands are in *trans* mutual positions, as usually found in similar Ir-complexes.[12, 15, 18] Bonding parameters are in keeping with those previously reported for related Ir(III) and Ru(II) complexes containing tetrazole ligands. [11, 12, 15, 18]

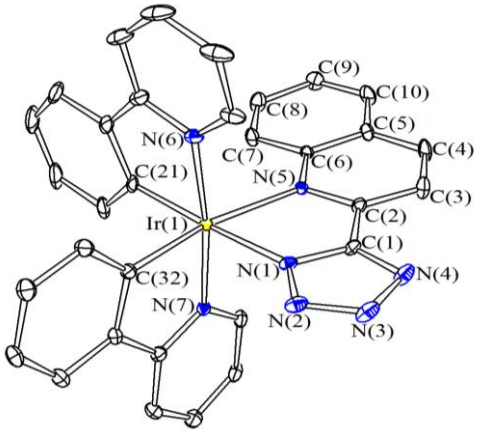

Figure 1. Molecular structure of **[IrQTZ]** with key atoms labeled. Hydrogen atoms have been omitted for clarity. Displacement ellipsoids are at the 30% probability level. Selected bond lengths (Å) and angles (deg): Ir(1)-N(1) 2.108(2), Ir(1)-N(5) 2.2873(19), Ir(1)-N(6) 2.044(2), Ir(1)-N(7) 2.039(2), Ir(1)-C(21) 2.012(3), Ir(1)-C(32) 2.004(2), N(1)-N(2) 1.346(3), N(2)-N(3) 1.316(3), N(3)-N(4) 1.359(3), C(1)-N(1) 1.329(3), C(1)-N(4) 1.333(3), C(1)-C(2) 1.458(3), N(6)-Ir(1)-N(7) 172.33(8), N(1)-Ir(1)-N(5) 75.10(7).

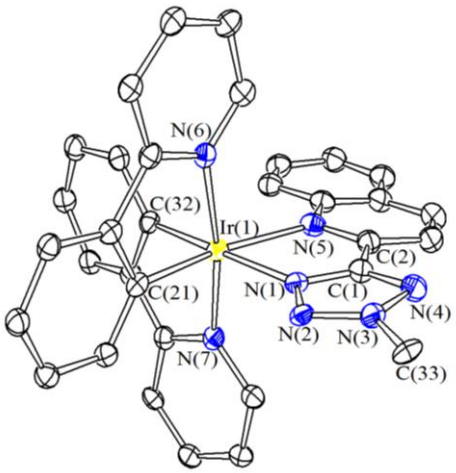

Figure 2. Molecular structure of **[IrQTZ-Me]**$^{+}$ with key atoms labeled. Hydrogen atoms have been omitted for clarity. Displacement ellipsoids are at the 30% probability level. Selected bond lengths (Å) and angles (deg): Ir(1)-N(1) 2.082(15), Ir(1)-N(5) 2.291(16), Ir(1)-N(6) 2.058(15), Ir(1)-N(7) 2.017(16), Ir(1)-C(21) 2.026(19), Ir(1)-C(32) 1.992(19), N(1)-N(2) 1.391(19), N(2)-N(3) 1.318(19), N(3)-N(4) 1.34(2), C(1)-N(1) 1.33(2), C(1)-N(4) 1.40(2), C(1)-C(2) 1.47(3), C(33)-N(3) 1.49(2), N(6)-Ir(1)-N(7) 171.1(6), N(1)-Ir(1)-N(5) 73.7(6).

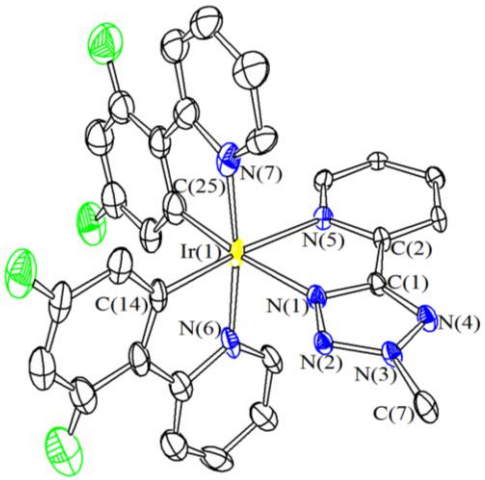

Figure 3. Molecular structure of **[F_2IrPTZ-Me]**$^{+}$ with key atoms labeled. Hydrogen atoms have been omitted for clarity. Displacement ellipsoids are at the 30% probability level. Selected bond lengths (Å) and angles (deg): Ir(1)-N(1) 2.127(11), Ir(1)-N(5) 2.184(10), Ir(1)-N(6) 2.048(8), Ir(1)-N(7) 2.022(8), Ir(1)-C(14) 2.010(7), Ir(1)-C(25) 2.042(8), N(1)-N(2) 1.329(14), N(2)-N(3) 1.315(14), N(3)-N(4) 1.337(14), C(1)-N(1) 1.329(16), C(1)-N(4) 1.329(17), C(1)-C(2) 1.457(16),C(7)-N(3) 1.465(16), N(6)-Ir(1)-N(7) 172.0(4), N(1)-Ir(1)-N(5) 76.2(4).

Photophysical properties

Even though the absorption and emission data of the quinoline based complexes **[IrQTZ]** and **[IrQTZ-Me]$^+$** have been described previously,[16] their photophysical properties are discussed and compared to those of the neutral fluorinated complex **[F_2IrPTZ]** and the corresponding cationic species **[F_2IrPTZ-Me]$^+$** measured in the same experimental conditions.

Table 1: Relevant absorption and emission data of neutral and cationic Ir(III) complexes discussed in this work.

CH_2Cl_2 as solvent	***Absorption***	***Emission 298 K[a,b]***					***Emission 77K[c]***	
	λ_{abs}(nm);($10^{-4}\varepsilon$)($M^{-1}cm^{-1}$)	λ_{em} (nm)	τ_{air} (µs)	τ_{Ar} (µs)	φ_{air} (%)	φ_{Ar} (%)	λ_{em} (nm)	τ (µs)
[IrQTZ]	260 (6.48), 342 (1.60), 386 (0.72), 423 (0.45)	580	0.160	0.840	2.6	6.5	516, 550	4.2
[IrQTZ-Me]$^+$	253 (4.25), 310 (1.41), 374 (0.78)	638	0.220	0.550	2.8	4.5	568	1.56
[F_2IrPTZ]	252 (7.84), 304 (3.30), 369 (1.04)	456, 486	0.100	0.160	2.8	6.9	456, 486	2.69
[F_2IrPTZ-Me]$^+$	257 (6.24), 318 (2.70), 351 (1.20)	454, 486, 526	0.040	0.140	1.7	4.7	448 480	6.62

[a]: "Air" means air equilibrated solutions, "Ar" means deoxygenated solutions under argon atmosphere; [b]: $[Ru(bpy)_3]Cl_2/H_2O$ was used as reference for quantum yield determinations (Φ_r = 0.028)[21]; [c]: in frozen CH_2Cl_2

The neutral and the cationic Ir(III) complexes display very similar absorption profiles, which consist of intense Ligand centred (LC) transitions in the higher energy part of the spectra (up to 300 nm) accompanied by weaker Metal-to-Ligand Charge Transfer (MLCT) processes at longer wavelengths (Figure 4) . Conversely, a dramatically different picture is drawn when the analysis of the emission properties is performed. As we demonstrated earlier,[11-15] indeed, tetrazolate- and tetrazole-based ligands induce a significant influence in determining the photoluminescent output of the corresponding neutral Ir(III) complexes. The occurrence of a similar behaviour is observed also for the complexes described herein.

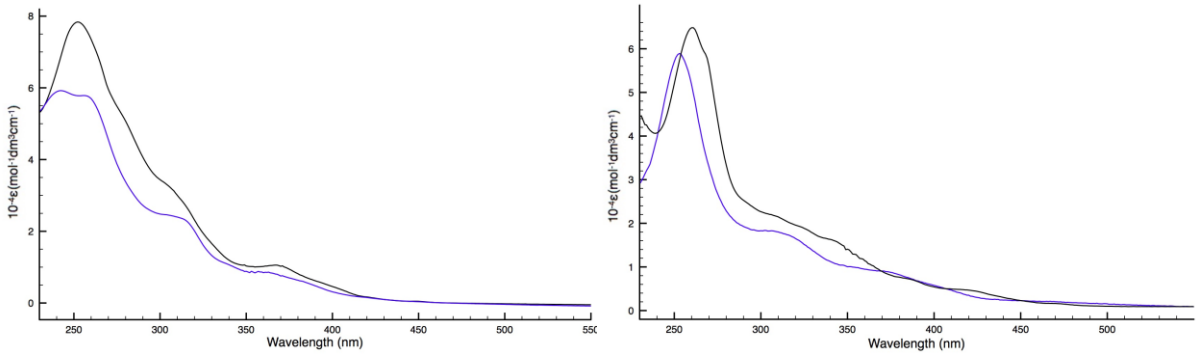

Figure 4: (left) Absorption profile of **[F_2IrPTZ]** (black line) and **[F_2IrPTZ-Me]$^+$** (blue line); (right) Absorption profile of **[IrQTZ]** (black line) and **[IrQTZ-Me]$^+$** (blue line), 10^{-5}M, CH_2Cl_2, r.t.

Upon excitation of the corresponding dilute dichloromethane solutions, the neutral complexes **[F_2IrPTZ]** and **[IrQTZ]** display wavelength independent and intense blue-sky (λ = 460, 490 nm, Fig. 5 and table 1) or orange (λ = 580 nm, Figure 5 and table 1) emissions, respectively, originating from the excited states of the triplet character. This assignment was supported by the oxygen sensitivity of the quantum yield (ϕ) and lifetime (τ) values (Table 1).

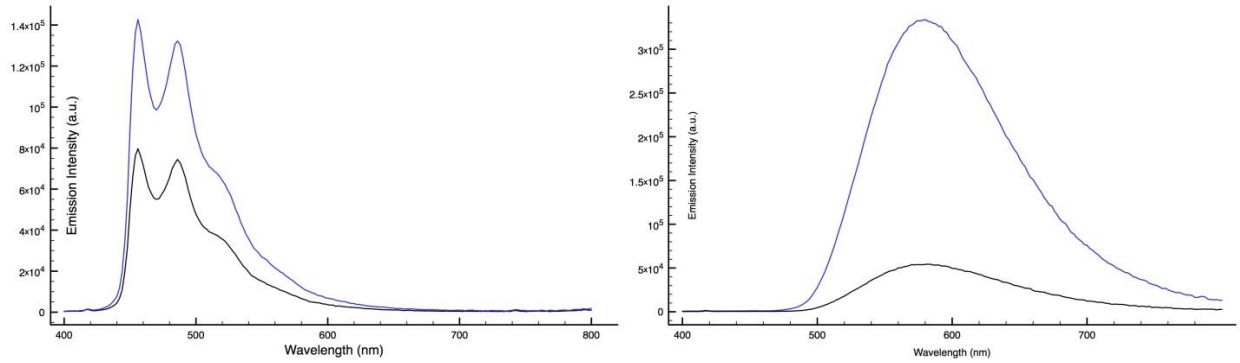

Figure 5: (left) Emission profile of **[F_2IrPTZ]**, air-equilibrated (black line) and deoxygenated solution (blue line) 10^{-5}M, CH_2Cl_2, r.t.; (right) Emission profile of **[IrQTZ]**, air-equilibrated (black line) and deoxygenated solution (blue line) 10^{-5}M, CH_2Cl_2, r.t.

In the case of **[F_2IrPTZ]**, the emission profile appears strongly structured. The presence of vibronic progressions is representative of the interplay of ^{3}LC/^{3}MLCT type emissive excited states, with the likely prevalent contribution of the ^{3}LC states over the ^{3}MLCT states suggested by the rather small rigidochromic blue shift that was encountered at 77 K (Figure 6, left).[1, 12a] Compared to **[F_2IrPTZ]**, the quinolyl tetrazolate based complex **[IrQTZ]** exhibited a red-shifted emission that is rationalised by the increased π conjugation on passing from a pyridyl to a quinolyl substituent. Also, as we have demonstrated earlier on the basis of experimental evidences and TD-DFT calculations,[12a, 16] this red shift suggests that the π* system of the quinolyl tetrazolato ligand acts as an electron

acceptor in the ^{3}MLCT charge transfer transitions, whose almost exclusive occurrence was witnessed by the broad and structureless emission profile and by the evident rigidochromic blue shift that was encountered on passing at 77K (Figure 6, right).[1, 12, 16]

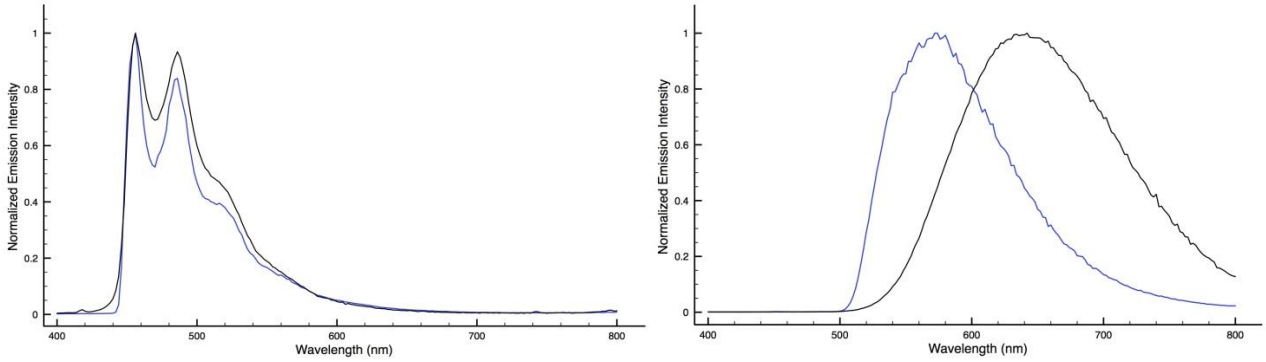

Figure 6: (left) Normalized emission profile of **[F$_2$IrPTZ]**, 298K (black line) and 77K (blue line); (right) Normalized emission profile of **[IrQTZ]**, 298K (black line) and 77K (blue line).

The conversion of the neutral **[F$_2$IrPTZ]** and **[IrQTZ]** into the corresponding methylated and positively charged Ir(III) complexes **[F$_2$IrPTZ-Me]$^+$** and **[IrQTZ-Me]$^+$**, respectively, involved the further modification of their luminescent output. Similarly to what we have previously observed for neutral Ir(III)-tetrazolato complexes, [12a, 15, 16] the addition of a methyl substituent to the coordinated tetrazolate ring was accompanied in both cases by the further red shift of the whole emission spectrum, which retained the vibronically structured profile, as for **[F$_2$IrPTZ-Me]$^+$**, or broad and featureless shape, as for **[IrQTZ-Me]$^+$** (Figure 7).

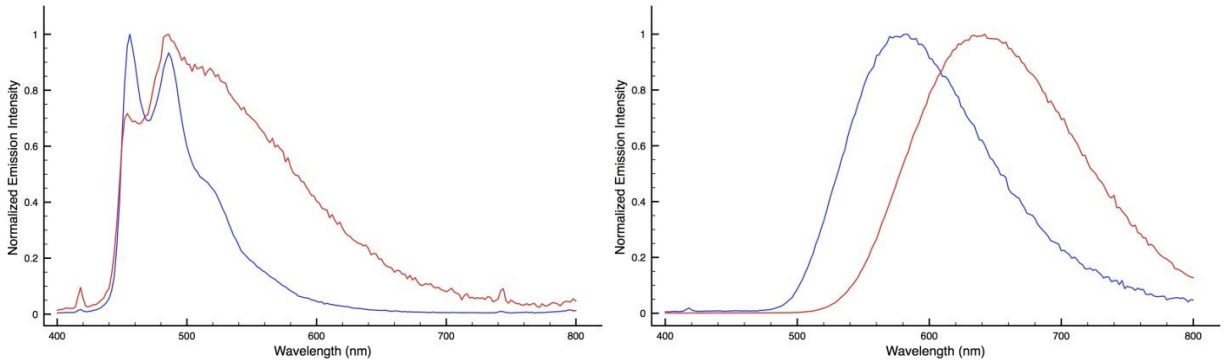

Figure 7: (left) Normalized emission profile of **[F$_2$IrPTZ]**, (blue line) and **[F$_2$IrPTZ-Me]$^+$** (red line); (right) Normalized emission profile of **[IrQTZ]**, (blue line) and **[IrQTZ-Me]$^+$** (red line).

Biological activity – antimicrobial properties

Inspired by the recent reports by the groups of Chao[10] and Crowley,[6a] we wanted to assess whether or not the conversion of neutral Ir(III) tetrazolates into cationic Ir(III) tetrazole complexes might confer any eventual antimicrobial activity, to be evaluated against Gram negative (*Escherichia coli*) and Gram positive bacteria (*Deinococcus radiodurans*).

The effect of the neutral and cationic Ir(III) complexes on bacterial growth was initially screened by performing disk diffusion tests in which ampicillin was used as the positive control. The appearance of inhibition zones around the paper disks soaked with solutions of the metal complexes was examined after incubation of the agar plates at 303 K for a period of 24 hours. As shown in Figure 8, none of the neutral or cationic Ir(III) complexes, which all display phosphorescent emission originating from excited states with triplet multiplicity, can inhibit the growth of *E. coli*, as no discernible inhibition zone did appear.

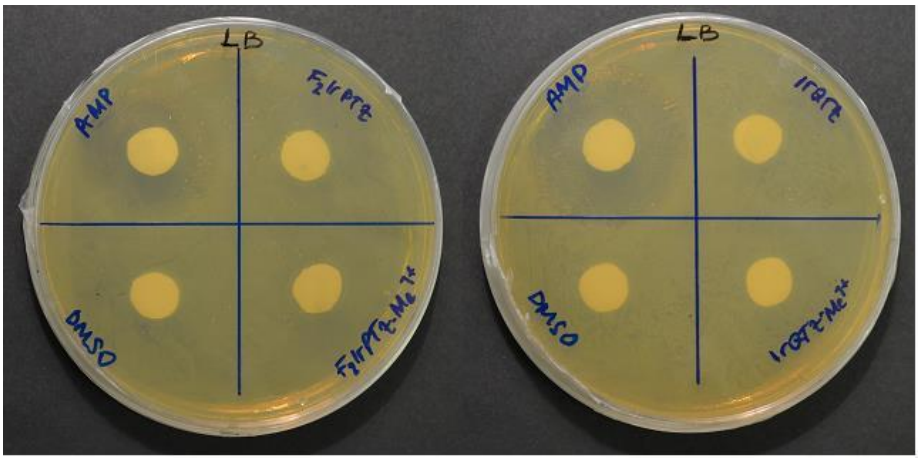

Figure 8: Disk diffusion tests against *E. coli* of **[F_2IrPTZ]** and **[F_2IrPTZ-Me]$^+$** (left, 20 μM) and against **[IrQTZ]** and **[IrQTZ-Me]$^+$** (right, 20 μM). Ampicillin ("AMP") was use as positive control (100 μg/mL).

A quite different outcome was observed when the same experiments were performed with *D. radiodurans*. Although the neutral complexes **[F_2IrPTZ]** and **[IrQTZ]** did not induce any detectable effect, clearly visible zones of inhibition were observed around the paper disks impregnated with **[F_2IrPTZ-Me]$^+$** and **[IrQTZ-Me]$^+$** cationic complexes (Figure 9). Following a closer inspection of the agar plates, it appeared that the cationic complex **[F_2IrPTZ-Me]$^+$** might induce a stronger effect than **[IrQTZ-Me]$^+$**. The inhibition zone surrounding the disk soaked with **[F_2IrPTZ-Me]$^+$** was indeed larger than that impregnated with the **[IrQTZ-Me]$^+$** cationic complex.

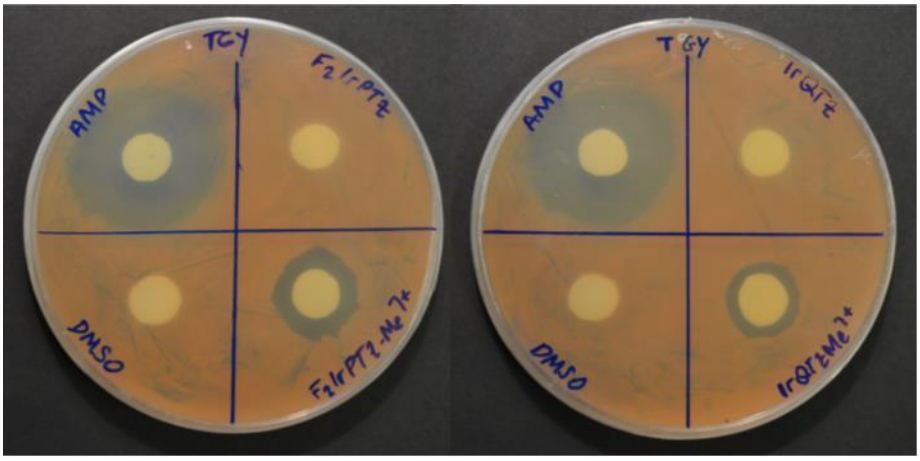

Figure 9: Disk diffusion tests against *D. radiodurans* of **[F$_2$IrPTZ]** and **[F$_2$IrPTZ-Me]$^+$** (left, 20 μM) and against **[IrQTZ]** and **[IrQTZ-Me]$^+$** (right, 20 μM). Ampicillin ("AMP") was used as positive control (100 μg/mL).

In order to verify the results obtained from disk diffusion tests, the growth kinetics of cultures of *E. coli* and *D. radiodurans* grown in the presence of different concentrations (5 and 20 μM, obtained by the dilution of ca. 1.5 mM DMSO stock solutions) of each neutral and cationic Ir(III) complex were analysed and compared to a control culture for each bacterial strain. Also, the occurrence of any eventual inhibitory effect arising from the presence of DMSO (0.4 and 1.5% (v/v)) that was used to dissolve the complexes was evaluated by appropriate control samples.

The analysis of the growth kinetics trends provided results in excellent agreement with those arising from the disk diffusion tests. The growth of *E. coli* (Figure 10 a-b) was not inhibited by the presence of both the neutral **[F$_2$IrPTZ]**, **[IrQTZ]** and cationic **[F$_2$IrPTZ-Me]$^+$**, **[IrQTZ-Me]$^+$** complexes, and all cultures showed comparable growth rates. Moreover, the presence of DMSO alone at low concentration, 0.4 or 1.5%, did not affect the growth rate of *E. coli* (see Figure 10).

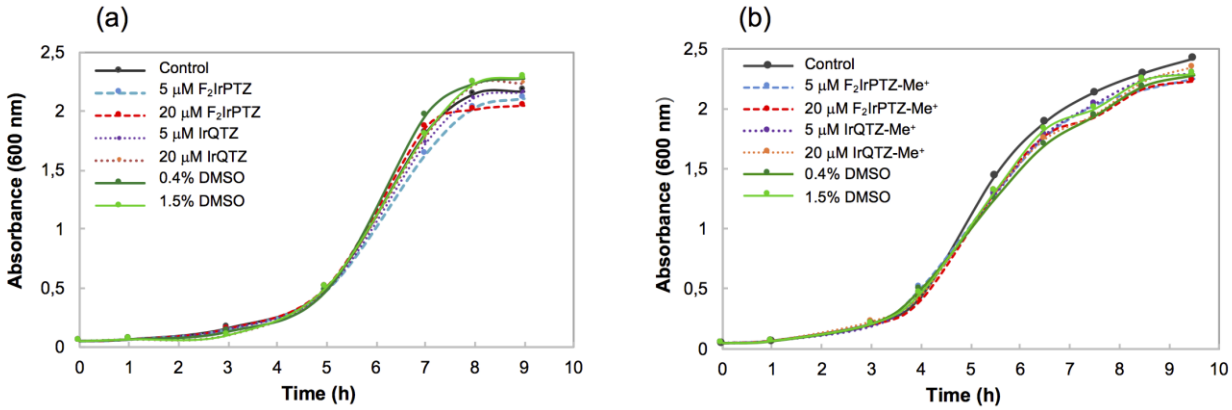

Figure 10: Kinetics of growth of *Escherichia coli* at 37 °C. Cultures were incubated with 5 µM and 20 µM **[F₂IrPTZ]** and **[IrQTZ]** or with 5 µM and 20 µM **[F₂IrPTZ-Me]⁺** and **[IrQTZ-Me]⁺** complexes (panel a and b, respectively). A control culture (dark dots) and cultures treated with 0.4% and 1.8% DMSO are shown (green and orange dots, respectively).

Similarly, the neutral complexes were found essentially devoid of any effect towards the growth of *D. radiodurans.* The only discrepancy in this trend was represented by the distinguishable decrease of the growth rate induced by the fluorinated complex **[F₂IrPTZ]** at the higher concentration value of 20 µM (Figure 11a), an effect that was no longer observed when the growth kinetics of *D. radiodurans* were analysed with respect to the neutral and not-fluorinated analogous complex **[Ir(PTZ)]**[12a] at the same concentration values (ESI, see Figure S31 and Table S6).

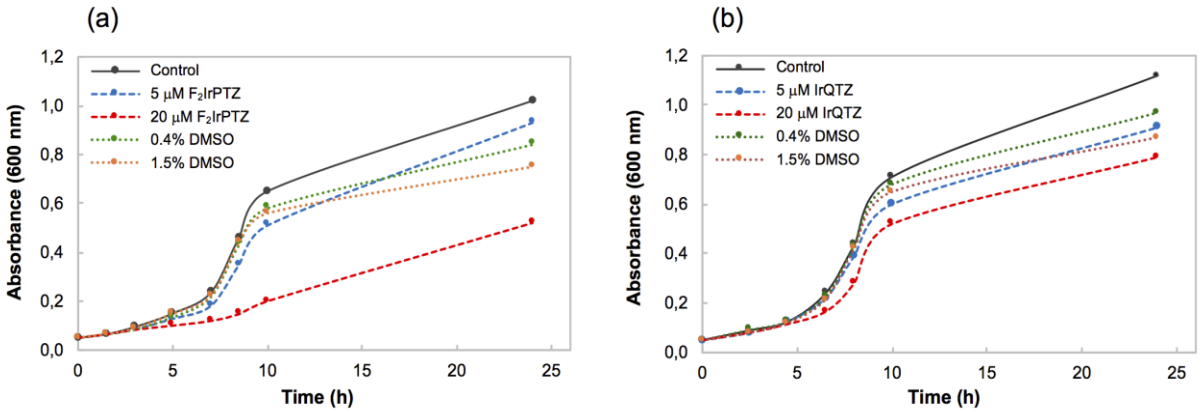

Figure 11: Kinetics of growth of *Deinococcus radiodurans* at 30 °C in the presence of neutral complexes. Cultures were treated with 5 µM and 20 µM **[F₂IrPTZ]** (a) or **[IrQTZ]** (b) (blue and red dots, respectively), 0.4% DMSO (green dots) and 1.5% DMSO (orange dots). A control culture without any complex was performed (black curve).

On the contrary, the growth of *D. radiodurans* cultures (Figure 12, a and b) appeared to be completely inhibited in the presence of the cationic complexes **[F$_2$IrPTZ-Me]$^+$** and **[IrQTZ-Me]$^+$**, with a significant antimicrobial activity triggered both by the 5 μM and 20 μM solutions of the complexes.

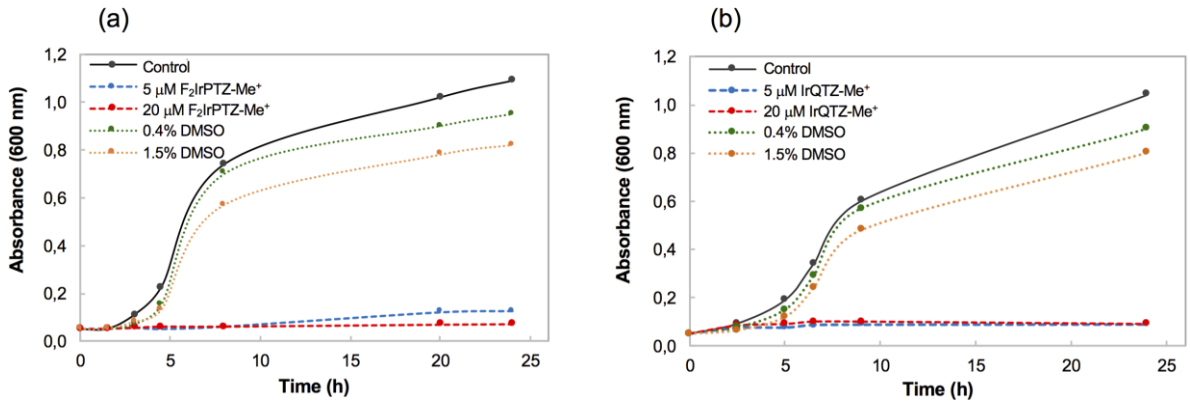

Figure 12: Kinetics of growth of *Deinococcus radiodurans* at 30 °C in the presence of cationic complexes. Cultures were treated with 5 μM and 20 μM **[F$_2$IrPTZ-Me]$^+$**(a) or **[IrQTZ-Me]$^+$**(b) (blue and red dots, respectively), 0.4% DMSO (green dots) and 1.5% DMSO (orange dots). A control culture without any complex was performed (black curve).

Moreover, further experiments were performed in order to get insights about the minimal inhibitory concentration (MIC) of the complexes. To this extent, the growth kinetics of *D. radiodurans* was measured upon exposing different bacterial cultures to **[F$_2$IrPTZ-Me]$^+$** and **[IrQTZ-Me]$^+$** complexes at concentration values ranging from 0.5 μM to 5 μM. At the lowest concentration limit (0.5 μM), both complexes appear essentially not active. On the contrary, the 1 μM solution of **[F$_2$IrPTZ-Me]$^+$** is effective, and completely inhibits the growth of *D. radiodurans*, while the **[IrQTZ-Me]$^+$** complex produces the same inhibition only at the upper concentration limit (5 μM), with an approximately linear decrease of the growth rate displayed by the intermediate concentration values (1.0 and 2.5 μM, Figure 13, a and b). Beyond suggesting the different MIC values for the cationic complexes, which correspond to MIC = 1 μg/mL for **[F$_2$IrPTZ-Me]$^+$** and 4 μg/mL for **[IrQTZ-Me]$^+$**, these results appear congruent with the different size of the inhibition zones that were observed in the agar disks diffusion tests (see Figure 9).

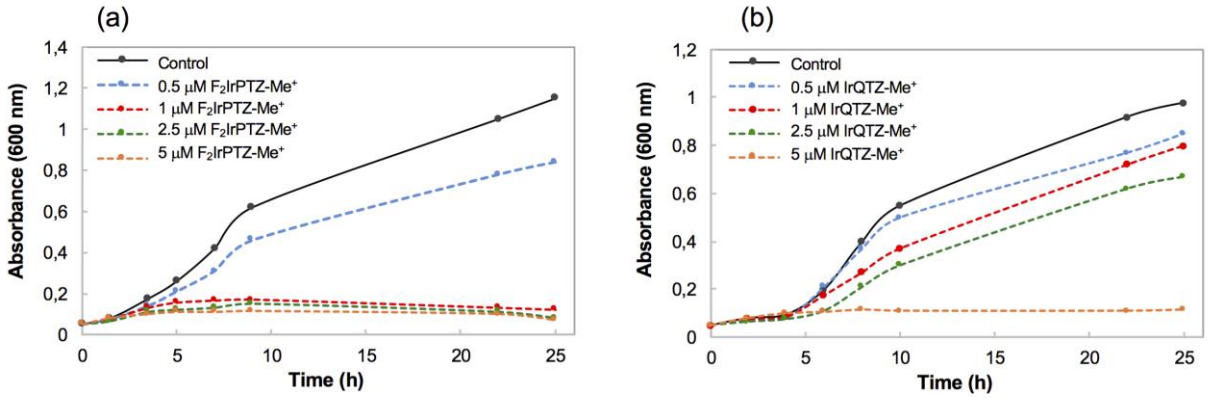

Figure 13: Kinetics of growth of *Deinococcus radiodurans* at 30 °C in the presence of different concentration of cationic complexes. Cultures were treated with 0.5, 1, 2.5 and 5 μM **[F_2IrPTZ-Me]$^+$** or **[IrQTZ-Me]$^+$** (a and b, respectively). A control culture without any complex was performed (black curve).

In summary, the analysis of the experimental evidences suggests how the antimicrobial activity of charge neutral Ir(III)-tetrazolate complexes described herein towards the Gram-positive *D. radiodurans* bacterium is promoted upon their conversion to the corresponding methylated cationic derivatives. Therefore, the presence of a positive net charge appears as the primary factor for determining the occurrence of inhibitory action by the cationic complexes **[F_2IrPTZ-Me]$^+$** and **[IrQTZ-Me]$^+$**. Further to their being consistent with the findings reported by the groups of Chao[10] and Crowley[6a] relative to inhibition of *S. aureus* growth by different sets of cationic Ir(III)cyclometalates and bis-cationic Ru(II)polypyridyls, our results suggest that the inhibition of the growth of *D. radiodurans* induced by the cationic Ir(III) complexes might be linked to their pronounced ability to disrupt the cell membrane of the Gram-positive *D. radiodurans*, while the dual membrane envelope present in the Gram-negative *E. coli* does most likely protect this bacterium from the cationic Ir(III) complexes. At this current stage, however, the occurrence of other mechanisms that might account for this particular behaviour cannot be excluded. In a recent report, indeed, Gimeno and coworkers[8b] suggested that the analogous specific selectivity to Gram-positive versus Gram-negative bacteria that is displayed by a set of cationic Ag(I)-aminophosphane complexes might be related to their inhibiting role in the peptidoglycan synthesis in the cell wall.

The occurrence of different MIC values for the charged species **[F_2IrPTZ-Me]$^+$** (MIC = 1 μg/mL), and **[IrQTZ-Me]$^+$** (MIC = 4 μg/mL), might be attributed to the differences in the structure of the cationic complexes. In particular, we suspect that the presence of fluorine substituents in the backbone of the cyclometalating ligands might play a not innocent role, as previously suggested by

the growth kinetics of *D. radiodurans* exposed to relatively high concentrations of the neutral **[F_2IrPTZ]** complex (Figure 11, a).

Finally, our results suggest that the antimicrobial properties of the Ir(III) complexes described herein might be independent from their luminescence features. In particular, the antimicrobial activity towards *E. coli* and *D. radiodurans* of the phosphorescent neutral and cationic Ir(III) complexes does not appear to be influenced in any way by the production of reactive oxygen species (ROS) such as singlet oxygen ($^1O_2$), under illumination with ambient light. In this regard, the growth kinetics of *D. radiodurans* in the presence of 5 μM and 20 μM solutions of **[F_2IrPTZ-Me]$^+$** and **[IrQTZ-Me]$^+$** were measured in dark conditions and provided results in excellent agreement with the previous experiments (ESI, see Figure S32 and Table S7).

Conclusions

The sensitivity to electrophilic additions that connotes the coordinated tetrazolate rings has been again demonstrated as a relatively simple, straightforward and powerful tool for the exploitment of the applicative opportunities of metal tetrazolate complexes. Indeed, the methylation of neutral and brightly luminescent cyclometalated Ir(III)tetrazolates involves their transformation into positively charged Ir(III) alkyl tetrazole complexes and the concomitant red shift of the corresponding emission colours.

Aiming at widening their applicative scenario, the families of neutral Ir(III) tetrazolates and cationic Ir(III)-tetrazole complexes were screened for any eventual antimicrobial activity *in vitro* against Gram negative (*E. coli*) and Gram positive (*D. radiodurans*) microorganisms. Whereas both kind of complexes were not active against *E. Coli*, the conversion of the neutral Ir(III) tetrazolates **[F_2IrPTZ]** and **[IrQTZ]** into the corresponding methylated and cationic Ir(III)tetrazole derivatives **[F_2IrPTZ-Me]$^+$** and **[IrQTZ-Me]$^+$** respectively, determined the turn-on of a good to excellent (MIC = 1 μg/mL for **[F_2IrPTZ-Me]$^+$** and 4 μg/mL for **[IrQTZ-Me]$^+$**) antimicrobial activity toward Gram positive *Deinococcus radiodurans*, a bacterium that – *albeit* not pathogenic – is listed as one of the toughest microorganisms in light of its outstanding resistance to radiation, oxidative stress and DNA damage. Thus, the occurrence of this behaviour, which we preliminary attribute to a membrane disruption effect induced by the positively charged Ir(III) tetrazole complexes, might constitute a promising platform for the development of metal tetrazole complexes as antimicrobial agents. In this context, we are addressing our future efforts to the investigation of other classes of luminescent tetrazolate/tetrazole complexes and to the further screening of their

antimicrobial potentialities with respect to pathogenic and antibiotic resistant Gram-positive bacterial strains such as methicillin resistant *Staphylococcus aureus* (MRSA).

Experimental section

General considerations. All the reagents and solvents were obtained commercially (Sigma Aldrich/Merck, Alfa Aesar, Strem Chemicals) and used as received without any further purification, unless otherwise specified. All the reactions were carried out under an argon atmosphere following Schlenk protocols. Where required, the purification of the Ir(III) complexes was performed via column chromatography with the use of Al_2O_3 as the stationary phase. ESI-mass spectra were recorded using a Waters ZQ-4000 instrument (ESI-MS, acetonitrile as the solvent). Nuclear magnetic resonance spectra (consisting of ^{1}H and ^{13}C) were always recorded using a Varian Mercury Plus 400 (^{1}H, 399.9; ^{13}C, 101.0 MHz). ^{1}H and ^{13}C chemical shifts were referenced to residual solvent resonances.

Photophysics. Absorption spectra were recorded at room temperature using a Perkin Elmer Lambda 35 UV/vis spectrometer. Uncorrected steady-state emission and excitation spectra were recorded on an Edinburgh FLSP920 spectrometer equipped with a 450 W xenon arc lamp, double excitation and single emission monochromators, and a Peltier-cooled Hamamatsu R928P photomultiplier tube (185−850 nm). Emission and excitation spectra were acquired with a cut-off filter (395 nm) and corrected for source intensity (lamp and grating) and emission spectral response (detector and grating) by a calibration curve supplied with the instrument. The wavelengths for the emission and excitation spectra were determined using the absorption maxima of the MLCT transition bands (emission spectra) and at the maxima of the emission bands (excitation spectra). Quantum yields (Φ) were determined using the optically dilute method by Crosby and Demas[19] at excitation wavelength obtained from absorption spectra on a wavelength scale [nm] and compared to the reference emitter by the following equation:[20]

$$\phi_s = \phi_r \left[\frac{A_r(\lambda_r)}{A_s(\lambda_s)}\right]\left[\frac{I_r(\lambda_r)}{I_s(\lambda_s)}\right]\left[\frac{n_s^2}{n_r^2}\right]\left[\frac{D_s}{D_r}\right]$$

where A is the absorbance at the excitation wavelength (λ), I is the intensity of the excitation light at the excitation wavelength (λ), n is the refractive index of the solvent, D is the integrated intensity of the luminescence, and Φ is the quantum yield. The subscripts r and s refer to the reference and the sample, respectively. A stock solution with an absorbance > 0.1 was prepared, then two dilutions were obtained with dilution factors of 20 and 10, resulting in absorbances of about 0.02 and 0.08 respectively. The Lambert-Beer law was assumed to remain linear at the concentrations of the solutions. The degassed measurements were obtained after the solutions were bubbled for 10 minutes under Ar atmosphere, using a septa-sealed quartz cell. Air-

equilibrated $[Ru(bpy)_3]Cl_2/H_2O$ solution (Φ = 0.028)[21] was used as reference. The quantum yield determinations were performed at identical excitation wavelengths for the sample and the reference, therefore deleting the I(λr)/I(λs) term in the equation. Emission lifetimes (τ) were determined with the single photon counting technique (TCSPC) with the same Edinburgh FLSP920 spectrometer using pulsed picosecond LED (EPLED 360, FWHM < 800ps) as the excitation source, with repetition rates between 1 kHz and 1 MHz, and the above-mentioned R928P PMT as detector. The goodness of fit was assessed by minimizing the reduced χ2 function and by visual inspection of the weighted residuals. To record the 77 K luminescence spectra, the samples were put in quartz tubes (2 mm diameter) and inserted in a special quartz Dewar filled with liquid nitrogen. The solvent used in the preparation of the solutions for the photophysical investigations was of spectrometric grade. Experimental uncertainties are estimated to be ±8% for lifetime determinations, ±20% for quantum yields, and ±2 nm and ±5 nm for absorption and emission peaks, respectively.

Ligand synthesis

Warning! Tetrazole derivatives are used as components for explosive mixtures.[22] In this lab, the reactions described here were only run on a few grams scale and no problems were encountered. However, great caution should be exercised when handling or heating compounds of this type.

Following the general method reported by Koguro and co-workers,[23] tetrazole ligands [H-**PTZ**] and [H-**QTZ**] has been obtained in quantitative yield.

[H-**PTZ**] **^{1}H-NMR** (DMSO *d*^{6}, 400 MHz) δ (ppm) = 8.77 (d, 1H, $J_{H–H}$ = 5.6 Hz), 8.20 (d, 1H, $J_{H–H}$ = 8 Hz) 8.07–8.03 (m, 1H), 7.62–7.59 (m, 1H). **^{13}C-NMR**, 100 MHz, DMSO-d^6 δ (ppm) = 155.3 (Ct), 150.5, 144.1, 138.7, 126.6, 123.1. [H-**QTZ**] **^{1}H-NMR**, (DMSO-*d*^{6}, 400 MHz) δ (ppm) = 8,65 (d, 1H, J_{H-H} = 8.79 Hz), 8,31 (d, 1H, J_{H-H} = 8.40 Hz), 8,17 (d, 1H, J_{H-H} = 8.40 Hz), 8,12 (d, 1H, J_{H-H} = 7.99 Hz), 7,90 (t, 1H), 7.74 (t, 1H);

General Procedure for the Preparation of the Neutral Ir(III) complexes

To a 3:1 solution of DCM/EtOH (15 mL) were added the dichloro-bridged Ir(III) dimer $[Ir(C\hat{}N)_2Cl]_2$ (1 eq) and 2.5 eq of [H-PTZ] or [H-QTZ]. The solution was stirred at r.t., for 6h. The solvent was removed by rotary-evaporation and the crude was subsequently purified with Al_2O_3 column chromatography eluted with a 8:2 DCM/acetone mixture, yielding the desired neutral Ir(III) complex (second fraction).

[F_2IrPTZ] **^{1}H-NMR** (CD_3CN, 400 MHz) δ (ppm): 8.38-8.36 (m, 1H); 8.32-8.29 (m, 2H); 8.11-8.07 (m, 1H); 7.90-7.86 (m, 3H); 7.67-7.65 (m, 1H); 7.59-7.56 (m, 1H); 7.41-7.37 (m, 1H); 7.12-7.05 (m, 2H); 6.72-6.60 (m, 2H); 5.86-5.83 (m, 1H); 5.78-5.75 (m, 1H). **^{13}C-NMR** (CD_3CN, 100 MHz) δ (ppm) = **ESI-MS** (*m/z*): $[M+H]^+$ = 720 m/z; $[M+Na]^+$ = 742 m/z; $[M+K]^+$ = 758 m/z. **^{13}C-NMR** (CD_3CN, 100 MHz) δ (ppm) = 164.86, 164.17, 164.00, 163.93, 163.86, 162.59, 162.22, 162.08, 161.64, 161.51, 160.13, 160.01, 159.64, 159.51, 156.42, 156.35, 152.17, 157.11, 150.50, 149.75, 149.44, 148.71, 139.98, 139.07, 138.93. Anal. Calcd. For $C_{28}H_{16}IrN_7F_4$ (718.68) C 46.8, H 2.24, N 13.64. Found: C 46.34, H 2.24, N 13.21.

[IrQTZ] **^{1}H-NMR** (CD_3CN, 400 MHz) δ (ppm): 8.61 – 8.53 (m, 2H), 8.06 – 8.00 (m, 2H), 7.97 – 7.92 (m, 2H), 7.89 – 7.87 (m, 1H), 7.81 – 7.68 (m, 4H), 7.53 – 7.49 (m, 1H), 7.33 – 7.32 (m, 1H), 7.19 – 7.15 (m, 1H), 7.06 – 7.02 (m, 1H), 6.99 – 6.93 (m, 3H), 6.90 – 6.87 (m, 1H), 6.83 – 6.79 (m, 1H), 6.49 – 6.48 (m, 1H), 6.15 – 6.13 (m, 1H). **^{13}C-NMR** (CD_3CN, 100 MHz) δ (ppm) = 169.45, 168.55, 166.76 (Ct), 157.09, 155.48, 152.50, 151.96, 150.26, 149.05, 146.01, 145.18, 145.07, 142.16, 139.34, 139.27, 133.48, 132.33, 131.45, 130.82, 130.75, 130.26, 129.12, 129.11, 126.29, 126.17, 125.51, 124.59, 124.34, 123.25, 123.23, 121.20, 120.76. **ESI-MS** (*m/z*): $[M+H]^+$ = 698 m/z. Crystals suitable for X-ray analysis (identified as **[IrQTZ]**·$3CH_3CN$, $C_{38}H_{31}IrN_{10}$) were obtained by slow diffusion of the complex in acetonitrile. Anal. Calcd. For $C_{38}H_{31}IrN_{10}$ (819.93) C 55.67, H 3.81, N 17.08. Found: C 55.81, H 3.95, N 17.23.

General Procedure for the Preparation of the Cationic Ir(III) complexes

1 eq of the desired neutral Ir(III) tetrazolate complex was added to dichloromethane and the mixture was allowed to cool down by immersion into an ethanol/liquid nitrogen cold bath. Then, methyl trifluoromethanesulfonate (1.2 equiv., solution in dichloromethane 0.179 M) was added. The reaction was stirred under nitrogen for 30 minutes while being kept in the cold bath, and then allowed to warm up to room temperature and stirred for 3 hours. Anion exchange was carried out by adding an excess of NH_4PF_6 in water to the solution and stirring for 20 minutes. The product was then extracted using dichloromethane (3×10 mL) and the organic components were combined and dried over anhydrous $MgSO_4$. Subsequent purification by column chromatography on alumina (gradient: CH_2Cl_2/acetone 8:2, second fraction) yielded 0.059 g of **[F_2IrPTZ-Me]$^+$[PF_6]$^-$** and 0.067 g of **[IrQTZ-Me]$^+$[PF_6]$^-$**.

[IrQTZ-Me]$^+$ ^{1}H-NMR (Acetone-d^6, 400 MHz) δ (ppm): 8.98 (d, 1H, J_{H-H} = 8.39 Hz), 8.67 (d, 1H, J_{H-H} = 8.39 Hz), 8.27 (d, 1H, J_{H-H} = 7.99 Hz), 8.19 – 8.07 (m, 4H), 8.01 – 7.83 (m, 5H), 7.73 (m, 1H), 7.37 (m, 1H), 7.10 – 6.98 (m, 5H), 6.86 (m, 1H), 6.44 (d, 1H, J_{H-H} = 7.59 Hz), 6.18 (d, 1H, J_{H-H} = 7.59 Hz), 4.59 (s, 3H). **^{13}C-NMR** (Acetone-d^6, 100 MHz) δ (ppm) = 167.93 (Ct), 167.69, 167.15, 151.08, 149.91, 149.61, 147.95, 146.63, 144.35, 143.83, 142.34, 140.12, 138.84, 138.80, 132.22, 131.63, 131.04, 130.66, 130.40, 129.78, 129.46, 129.37, 128.12, 125.15, 124.46, 123.76, 123.28, 122.73, 122.63, 120.04, 119.87, 119.72, 41.62. **ESI-MS** (*m/z*): [M$^+$] = 712 m/z [M$^-$] = 145 m/z (PF_6). Crystals suitable for X-ray analysis (identified as **[IrQTZ-Me]$^+$[PF$_6$]$^-$·solv**, $C_{33}H_{25}F_6IrN_7P$) were obtained by slow diffusion of the complex in dichloromethane. Anal. Calcd. For $C_{33}H_{25}F_6IrN_7P$ (856.77) C 46.26, H 2.94, N 11.44. Found: C 40.95, H 2.85, N 9.55.

[F$_2$IrPTZ-Me]$^+$ ^{1}H-NMR (CD_3CN, 400 MHz) δ (ppm): 8.46-8.44 (d, 1H, J_{H-H} = 8.00 Hz); 8.36-8.33 (d, 2H, J_{H-H} = 8.80 Hz); 8.26-8.23 (m, 1H); 8.02-7.95 (m, 3H); 7.87-7.86 (d, 1H, J_{H-H} = 5.20 Hz); 7.66-7.63 (m, 2H); 7.17-7.12 (m, 2H); 6.79-6.69 (m, 2H); 5.75-5.73 (m, 2H); 4.47 (s, 3H). **^{13}C-NMR** (CD_3CN, 100 MHz) δ (ppm): 166.54, 164.69, 164.57, 164.13, 164.00, 163.60, 163.53, 163.27, 163.20, 162.59, 162.08, 162.02, 161.95, 161.47, 159.88, 159.50, 151.76, 151.71, 151.47, 151.30, 151.23, 150.43, 150.37, 150.05, 149.97, 149.61, 148.40, 148.32, 144.02, 140.94, 140.80, 140.77, 139.80, 139.62, 139.36, 139.32, 129.93, 129.83, 128.20, 124.84, 124.77, 124.74, 42.08. **ESI-MS** (*m/z*): [M] $^+$ = 734 m/z [M] $^-$ = 145 m/z (PF_6). Crystals suitable for X-ray analysis (identified as **[F$_2$IrPTZ-Me]$^+$[PF$_6$]$^-$·2CH$_2$Cl$_2$**, $C_{31}H_{23}Cl_4F_{10}IrN_7P$) were obtained by slow diffusion of the complex in dichloromethane. Anal. Calcd. For $C_{31}H_{23}Cl_4F_{10}IrN_7P$ (1048.53) C 35.51, H 2.21, N 9.35. Found: C 35.73, H 2.46, N 9.93.

Bacterial strains and media

The Gram-negative *Escherichia coli* TOP10 strain (Invitrogen) was cultivated in Luria-Bertani (LB) medium (1% Tryptone, 0.5% yeast extract, 1% NaCl). Solid plates were prepared by adding 1.5% agar. *Deinococcus radiodurans*, a red-pigmented Gram-positive bacterium, was grown in TGY medium (0.5% Tryptone, 0.1% glucose, 0.3% yeast extract), to which 1.5% of agar was added if necessary.

Disk diffusion test

A dilution (0.1 mL) of a liquid overnight culture (corresponding to approximately 1x10^8 CFU/mL) was spread on LB and TGY agar plates in order to produce bacterial lawns. Filter paper disks

impregnated with ampicillin (100 μg/mL), **[F$_2$IrPTZ]**, **[IrQTZ]**, **[F$_2$IrPTZ-Me]$^+$**, **[IrQTZ-Me]$^+$**, all at conecentration of 20 μM,and DMSO were placed on the surface of agar plates. After incubation for 24 h at 30 °C (*D. radiodurans*) and 37 C° (*E. coli*), the presence of inhibition zones was determined and measured. Ampicillin was used as positive control of antimicrobial activity.

Bacterial growth curves

To prepare the inoculum of *E. coli*, a single colony was inoculated in 2 mL LB medium and cultivated at 37 °C under shaking for 15 h. The overnight pre-culture was diluted to 0.05 optical density at 600 nm (OD_{600nm}) into Falcon tubes containing 5 mL of fresh medium and the growth was measured at appropriate time intervals using a plastic cuvette in a spectrophotometer (GeneQuant, Amersham Pharmacia). For D. *radiodurans*, the inoculum was prepared by growing a single colony in 5 mL of TGY broth at 30 °C for 24 h in a shaker incubator. The pre-culture was diluted to 0.05 OD into 5 mL of fresh TGY medium and the cell growth at 30 °C was determined by reading the optical density at 600 nm with a spectrophotometer. 5 μM and 20 μM of **[F$_2$IrPTZ]**, **[IrQTZ]**, **[F$_2$IrPTZ-Me]$^+$** and **[IrQTZ-Me]$^+$** complexes were separately added to *E. coli* or *D. radiodurans* cultures. Control cultures treated with DMSO alone (0.4 and 1.5%) were performed.

Determination of MIC

Five cultures of *D. radiodurans* (5 mL TGY) were incubated with different dilutions of **[F$_2$IrPTZ-Me]$^+$** or **[IrQTZ-Me]$^+$** complexes in order to obtain final concentrations ranging from 0 to 5 μM. Dilutions were performed in DMSO. The rate of bacterial growth was measured as described before.

X-ray crystallography

Crystal data and collection details for **[IrQTZ]·3CH$_3$CN**, **[IrQTZ-Me]$^+$[PF$_6$]$^-$·solv** and **[F$_2$IrPTZ-Me]$^+$[PF$_6$]$^-$·2CH$_2$Cl$_2$** are reported in Table S8 (ESI). The diffraction experiments were carried out on a Bruker APEX II diffractometer equipped with a PHOTON100 (**[IrQTZ]·3CH$_3$CN**, and **[F$_2$IrPTZ-Me]$^+$[PF$_6$]$^-$·2CH$_2$Cl$_2$**) or a CCD (**[IrQTZ-Me]$^+$[PF$_6$]$^-$·solv**) detector and using Mo-K radiation. Data were corrected for Lorentz polarization and absorption effects (empirical absorption correction SADABS.[24] Structures were solved by direct methods and refined by full-matrix least squares based on all data using F^2.[25] H-atoms were placed in calculated positions, and refined isotropically using a riding model. All non-hydrogen atoms were refined with anisotropic displacement parameters, unless otherwise stated. One CH_3CN molecule of **[IrQTZ]·3CH$_3$CN** is disordered: this has been split

into two positions and refined using one occupancy factor per disordered group. Similar *U* restraints (SIMU line in SHELXL; s.u. 0.02) were applied to the CH_3CN molecules. The quality of the crystals of **[IrQTZ-Me]$^+$[PF$_6$]$^-$·solv** was very low. Thus, the data have been cut at 2 = 47.06° and the value of R_{int} is rather high, as evidenced by two ALERT A in the check-cif file. Once located the **[IrQTZ-Me]$^+$** cation and **[PF$_6$]$^-$** anion, some solvent accessible void remain within the unit cell after refinement. Because of the low quality of the crystals, it has not been possible to locate nor identify these solvent molecules. Thus, they have been treated using the SQUEEZE routine of PLATON.[26] All the C and N-atoms have been restrained to have similar *U* parameters (SIMU line in SHELXL; s.u. 0.01) and isotropic like behavior (ISOR line in SHELXL; s.u. 0.01). Despite the low quality of the structural data, the connectivity and overall geometry of the complex is rather reliable and comparable to similar structures. The C and N atoms of **[F$_2$IrPTZ-Me]$^+$[PF$_6$]$^-$·2CH$_2$Cl$_2$** have been restrained to have similar *U* parameters (SIMU line in SHELXL; s.u. 0.02), and the F atoms to have and isotropic like behavior (ISOR line in SHELXL; s.u. 0.005). The aromatic rings have been constrained to fit regular hexagons (AFIX 66 line in SHELXL). Some residual electron density (ALERT A in the check-cif file) remains after refinement close to the Ir atom in positions that are not realistic for any atom. These are series termination errors, which are common with heavy atoms such as Ir.

CCDC 1558752 for [IrQTZ]·3CH_3CN, 1558753 for [IrQTZ-Me]$^+$[PF_6]$^-$·solv and 1558753 for [F_2IrPTZ-Me]$^+$[PF_6]$^-$·2CH_2Cl_2 contain the supplementary crystallographic data for this paper.

Electronic Supporting Information (ESI) available: NMR (^{1}H, ^{13}C) and ESI-MS spectra of all the Ir(III) based species. Crystallographic data; UV-vis absorption, emission spectra recorded at r.t and 77K, kinetics of growth of *E. coli* and *D. radiodurans*.

Acknowledgements The authors wish to thank the Italian Ministry of Education, University and Research (MIUR) for financial support (PRIN project: Towards a Sustainable Chemistry: Design of Innovative Metal-Ligand Systems for Catalysis and Energy Applications). M.M. and A.M.R would like to thank the Australian Research Council for funding (FT130100033).

Graphical Abstract

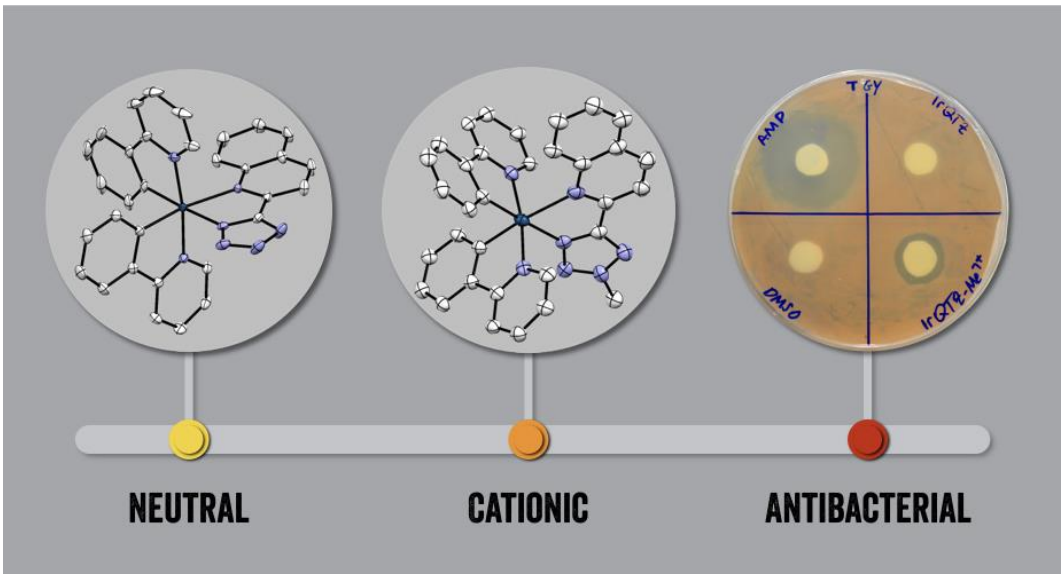

The conversion of neutral Ir(III) tetrazolate complexes into their cationic analogues induces the systematic red-shift of their emissions and the switch-on of their antibacterial properties against *Deinococcus radiodurans*, one of the more robust bacterium known.

References

[1] L. Flamigni, A. Barbieri, C. Sabatini, B. Ventura and F. Barigelletti, *Top. Curr. Chem.* 2007, **281**, 143-203.

[2] Highly Efficient OLEDs with Phosphorescent Materials, (Ed: H. Yersin), Wiley-VCH, Weinheim, Germany 2008.

[3] a) K. K.-W. Lo, K. H.-K. Tsang, K.-S. Sze, C.-K. Chung, T. K.-M. Lee, K. Y. Zhang, W.-K. Hui, C.-K. Li, J. S.-Y. Lau, D. C.-M. Ng and N. Zhu*, Coord. Chem. Rev.* 2007, **251**, 2292. b) K. K.-W. Lo, W.-K. Hui, C.-K. Chung, K. H.-K. Tsang, T. K.-M. Lee, C.-K. Li, J. S.-Y. Lau and D. C.-M. Ng, *Coord. Chem. Rev.* 2006, **250**, 1724. c) K. K.-W. Lo, W.-K. Hui, C.-K. Chung, K. H.-K. Tsang, D. C.-M. Ng, N. Zhu and K.-C. Cheung, *Coord. Chem. Rev.* 2005, **249**, 1434.

[4] D. M. Schultz and T. P. Yoon, *Science*, 2014, **343**, 1239176.

[5] a) K. K.-W. Lo and S. P.-Y. Li, *RSC Adv.*, 2014, **4**, 10560–10626; b) K. K.-W. Lo, D. Ng, and C. Chung, *Organometallics*, 2001, **20**, 4999–5001.

[6] a) S. V. Kumar, S. Ø. Scottwell, E. Waugh, C. J. McAdam, L. R. Hanton, H. J. L. Brooks and J. D. Crowley, *Inorg. Chem.*, 2016, **55**, 9767–9777.b) F. Li, J. G. Collins, F. R. Keene, *Chem. Soc. Rev.,* 2015, **44**, 2529−2542 and references cited therein; c) P.-L. Lam, G.-L. Lu, K.-M. Hon, K.-W. Lee, C.-L. Ho, X. Wang, J. C.-O. Tang, K.-H. Lam, R. S.-M. Wong, S. H.-L. Kok, Z.-X. Bian, H. Li, K. K.-H. Lee, R. Gambari, C.-H. Chui and W.-Y. Wong, *Dalton Trans.*, 2014, **43**, 3949–3957 d) N. L. Kilah and E. Meggers, *Aust. J. Chem.* 2012, **65**, 1325−1332; e) G. Karpin, J. S. Merola and J. O. Falkinham III, *Antimicrob. Agents Chemother.*, 2013, **57**, 3434–3436; f) M. Pandrala, F. Li, M. Feterl, Y. Mulyana, J. M. Warner, L. Wallace, F. R. Keene and J. G. Collins, *Dalton Trans.*, 2013, **42**, 4686–4694.

[7] a) J. A. Lemire, J. J. Harrison and R. J. Turner, *Nature Reviews Microbiology*, 2013, **11**, 371–384; b) K. D. Mjos and C. Orvig, *Chem. Rev.*, 2014, **114**, 4540−4563; c) M. Patra, G. Gasser and N. Metzler-Nolte, *Dalton Trans.*, 2012, **41**, 6350–6358.

[8] a) S. Medici, M. Peana, G. Crisponi, V. M. Nurchi, J. I. Lachowicz, M. Remelli and M. A. Zoroddu, *Coord. Chem Rev.*, 2016, **327**-**328**, 349-359 and references cited therein; b) L. Ortego, J. Gonzalo-Asensio, A. Laguna, M.D. Villacampa and M.C. Gimeno, *J. Inorg. Biochem.*, 2015, **146**, 19–27;c) F. Hackenberg and M. Tacke, *Dalton Trans.*, 2014, **43**, 8144–8153.

[9] a) G. W. Karpin, D. M. Morris, M. T. Ngo, J. S. Merola and J. O. Falkinham III, *Med. Chem. Commun.*, 2015, **6**, 1471–1478; b) P. V. Simpson, C. Schmidt, I. Ott, H. Bruhn and U. Schatzschneider, *Eur. J. Inorg. Chem.*, 2013, 5547–5554.

[10] L. Lu, L.–J. Liu, W.-C. Chao, H.-J. Zhong, M. Wang, X.–P. Chen, J.–J. Lu, R.-N Li, D.–L. Ma and C.–H. Leung, *Sci. Rep.*, 2015, **5**, 14544.

[11] a) S. Stagni, E. Orselli, A. Palazzi, L. De Cola, S. Zacchini, C. Femoni, M. Marcaccio, F. Paolucci and S. Zanarini, *Inorg. Chem.,* 2007, **46**, 9126-9138; b) M. V. Werrett, D. Chartrand, Gale, J. D.G. S. Hanan, J. G. MacLellan, M. Massi, S. Muzzioli, P. Raiteri, B. W. Skelton, M. Silberstein and Stagni, S. *Inorg. Chem.,* 2011, **50**, 1229-1241; c) K. D. M. MaGee, P. J. Wright, S. Muzzioli, C. M. Siedlovskas, P. Raiteri, M. V. Baker, D. H. Brown, S. Stagni and M. Massi, *Dalton Trans.*, 2013, **42**, 4233–4236; d) C. A. Bader, E. A. Carter, A. Safitri, P. V. Simpson, P. Wright, S. Stagni, M. Massi, P. A. Lay, D. A. Brooks and S. E. Plush, *Mol. BioSyst.* 2016, **12**, 2064–2068; e) C. A. Bader, A. Sorvina, P. V. Simpson, P. J. Wright, S. Stagni, S. E. Plush, M. Massi and D. A. Brooks, *FEBS Letters* 2016, **590**, 3051–3060.

[12] a) S. Stagni, S. Colella, A. Palazzi, G. Valenti, S. Zacchini, F. Paolucci, M. Marcaccio, R. Q. Albuquerque and L. De Cola, *Inorg. Chem.*, 2008, **47**, 10509–10521; b) V. Fiorini, A. D'Ignazio, K. D. M. Magee, M. I. Ogden, M. Massi and S. Stagni, *Dalton Trans*., 2016, **45**, 3256-3259.

[13] M. V. Werrett, G. S. Huff, S. Muzzioli, V. Fiorini, S. Zacchini, B. W. Skelton, A. Maggiore, J. M. Malicka, M. Cocchi, K. C. Gordon, S. Stagni and M. Massi, *Dalton Trans*., 2015, **44**, 8379-8393.

[14] V. Fiorini, A. M. Ranieri, S. Muzzioli, K. D. M. Magee, S. Zacchini, N. Akabar, A. Stefan, M. I. Ogden, M. Massi and S. Stagni, *Dalton Trans.*, 2015, **44**, 20597-20608..

[15] M. V. Werrett, S. Muzzioli, P. J. Wright, A. Palazzi, P. Raiteri, S. Zacchini, M. Massi and S. Stagni, *Inorg. Chem.*, 2014, **53**, 229–243.

[16] C. Caporale, C. A. Bader, A. Sorvina, K. D. M. Magee, B. W. Skelton, P. J. Wright, P. Raiteri, S. Stagni, S. E. Plush, D. A. Brooks and M. Massi, *Chem. Eur. J.,* 2017, DOI: 10.1002/chem.201701352.

[17] a) D. Slade and M. Radman, *Microbiol. Mol. Biol. Rev.*, 2011, **75**, 133-191; b) L. Wei, M. Yun, X. Fangzhu, and H. Shuya, *Advances in Natural Science*, 2014, **7**, 6-14.

[18] V. Fiorini, S. Zacchini, P. Raiteri, R. Mazzoni, V. Zanotti, M. Massi and S. Stagni, *Dalton Tran*s., 2016, **45**, 12884-12896.

[19] G. A. Crosby and J. N. Demas, *J. Phys. Chem*. 1971, **75**, 991-1024.

[20] D. F. Eaton, *Pure Appl. Chem*. 1988, **60**, 1107-1114.

[21] K. Nakamura, *Bull. Chem. Soc. Jpn*. 1982, **55**, 2697–2705.

[22] R. N. Butler, Tetrazoles. In "Comprehensive Heterocyclic Chemistry II"; Storr, R. C., Ed.; Pergamon Press: Oxford, U.K., 1996; Vol. **4**, 621-678, and references cited therein.

[23] K. Koguro, T. Oga, S. Mitsui and R. Orita, *Synthesis*, 1998, 910-914.

[24] G. M. Sheldrick, *SADABS-2008/1 - Bruker AXS Area Detector Scaling and Absorption Correction*, Bruker AXS: Madison, Wisconsin, USA, 2008.

[25] G. M. Sheldrick, *Acta Crystallogr. C*, 2015, **71**, 3.

[26] a) A. L. Spek, *J. Appl. Cryst*. 2003, **36**, 7; b) A. L. Spek. *Acta Cryst*., 2009, **D65**, 148.